Autosomal Dominant *PTH* Gene Signal Sequence Mutation in a Family With Familial Isolated Hypoparathyroidism

Luigia Cinque,[1]* Angelo Sparaneo,[1]* Laura Penta,[2] Amedea Mencarelli,[3] Daniela Rogaia,[3] Susanna Esposito,[2] Federico Pio Fabrizio,[1] Filomena Baorda,[1] Alberto Verrotti,[4] Alberto Falorni,[5] Gabriela Stangoni,[3] Geoffrey N. Hendy,[6,7,8,9] Vito Guarnieri,[1] and Paolo Prontera[3]

[1]Medical Genetics and Laboratory of Oncology, IRCCS Casa Sollievo della Sofferenza Hospital, San Giovanni Rotondo, Foggia 71013, Italy; [2]Department of Pediatrics, University of Perugia, Perugia 06100, Italy; [3]Regional Reference Centre for Medical Genetics, "Santa Maria della Misericordia" Hospital, Perugia 06129, Italy; [4]Department of Paediatrics, University of L'Aquila, L'Aquila 67100, Italy; [5]Section of Internal Medicine and Endocrine and Metabolic Sciences, Department of Medicine, University of Perugia, Perugia 06100, Italy; [6]Metabolic Disorders and Complications, McGill University Health Centre Research Institute, Montreal, Quebec H4A 3J1, Canada; [7]Department of Medicine, McGill University, Montreal, Quebec H4A 3J1, Canada; [8]Department of Physiology, McGill University, Montreal, Quebec H3G 1Y6, Canada; and [9]Department of Human Genetics, McGill University, Montreal, Quebec H3A 0C7, Canada

Context: Familial isolated hypoparathyroidism (FIH) is a genetically heterogeneous disorder due to mutations of the calcium-sensing receptor (*CASR*), glial cells missing-2 (*GCM2*), guanine nucleotide binding protein α11 (*GNA11*), or parathyroid hormone (*PTH*) genes. Thus far, only four cases with homozygous and two cases with heterozygous mutations in the *PTH* gene have been reported.

Objective: To clinically describe an FIH family and identify and characterize the causal gene mutation.

Design: Genomic DNA of the family members was subjected to *CASR*, *GCM2*, *GNA11*, and *PTH* gene mutational analysis. Functional assays were performed on the variant identified.

Participants: Six subjects of a three-generation FIH family with three affected individuals having severe hypocalcemia and inappropriately low serum PTH.

Results: No mutations were detected in the *CASR*, *GCM2*, and *GNA11* genes. A heterozygous variant that segregated with the disease was identified in *PTH* gene exon 2 (c.41T>A; p.M14K). This missense variant, in the hydrophobic core of the signal sequence, was predicted *in silico* to impair cleavage of preproPTH to proPTH. Functional assays in HEK293 cells demonstrated much greater retention intracellularly but impaired secretion into the medium of the M14K mutant relative to wild type. The addition of the pharmacological chaperone, 4-phenylbutyric acid, led to a reduction of cellular retention and increased accumulation in the cell medium of the M14K mutant.

Conclusions: We report a heterozygous *PTH* mutation in an FIH family and demonstrate accumulation of the mutant intracellularly and its impaired secretion. An accurate genetic diagnosis in such hypoparathyroid patients is critical for appropriate treatment and genetic counseling. **(*J Clin Endocrinol Metab* 102: 3961–3969, 2017)**

ISSN Print 0021-972X ISSN Online 1945-7197
Printed in USA

Received 27 January 2017. Accepted 15 August 2017.
First Published Online 18 August 2017

*These authors contributed equally to this work.

Abbreviations: ADH, autosomal dominant hypocalcemia; *CASR*, calcium-sensing receptor; cDNA, complementary DNA; ER, endoplasmic reticulum; FIH, familial isolated hypoparathyroidism; *GCM2*, glial cells missing-2; *GNA11*, guanine nucleotide binding protein α11; HEK, human embryonic kidney; MIM, Mendelian Inheritance in Man; mRNA, messenger RNA; NR, normal range; PBA, 4-phenylbutyric acid; PCR, polymerase chain reaction; PTH, parathyroid hormone; WT, wild-type.

In primary hypoparathyroidism with hypocalcemia and hyperphosphatemia, deficient parathyroid hormone (PTH) secretion most commonly occurs from surgical excision of or damage to the parathyroid glands (1). Idiopathic hypoparathyroidism refers to isolated cases when a cause is not obvious and the family history is negative. However, hypoparathyroidism is also a feature common to a variety of hereditable syndromes (2). Familial isolated hypoparathyroidism (FIH) can present in an autosomal dominant or autosomal recessive fashion and can be due to mutations in the calcium-sensing receptor (*CASR*), glial cells missing-2 (*GCM2*), the G protein α11 (*GNA11*) or *PTH* genes (3).

Gain-of-function mutations in the *CASR* gene [Mendelian Inheritance in Man (MIM) no. 601199] have been identified in a number of families with a clinical diagnosis of autosomal dominant hypocalcemia (ADH) type 1 (MIM no. 601198). In the parathyroid gland, the activated CASR (the calciostat) suppresses PTH secretion, and, in the kidney, it induces hypercalciuria, which can contribute to the hypocalcemia. In many cases of ADH type 1, the family history is positive; however, *de novo* mutations are quite common (4, 5).

The Gα11 protein (a Gq family member; MIM no. 139313) couples the CASR to its downstream signaling pathways. Heterozygous gain-of-function missense mutations of *GNA11* have been found in the few patients with ADH type 2 (MIM no. 615361), without detectable *CASR*-activating mutations identified thus far (4, 5). The *GNA11*-activating mutations increase the sensitivity of the parathyroid gland and renal tubule to extracellular calcium concentrations.

The *GCM2* gene (MIM no. 603716) encodes a transcription factor expressed in the PTH-secreting cells of the developing parathyroid glands and is critical for their development in terrestrial vertebrates (6). Recessively and dominantly inherited FIH can occur with homozygous and heterozygous mutations of the *GCM2* gene, respectively (7–9), although their prevalence is not high in cases of isolated hypoparathyroidism (3).

In a few cases of FIH, mutations in the *PTH* gene (MIM no. 168450) have been implicated (Table 1). The preproPTH messenger RNA (mRNA) translated on rough endoplasmic reticulum (ER) polyribosomes encodes an amino-terminal 25-amino-acid signal or prepeptide (that directs the nascent chain into the ER, where it is cotranslationally cleaved by the signalase enzyme). This is followed by a 6-amino-acid propeptide that is removed by proprotein convertases, after trafficking to the Golgi apparatus, to generate the mature 84-amino-acid PTH polypeptide. In a family with autosomal recessive hypoparathyroidism, a homozygous signal sequence mutation (S23P) segregated with the disease (10). This mutation might prevent proper cleavage of the signal peptide during processing of the nascent protein. In a girl with isolated hypoparathyroidism, a homozygous S23X signal sequence mutation was found, predicting for a truncated inactive PTH peptide (11). A homozygous [Cys25]PTH(1-84) mutation that impairs activation of the PTH receptor 1 was identified in an idiopathic hypoparathyroid family (12). Elevated circulating PTH levels were found in some (but not all) assays, thus defining a novel form of hypoparathyroidism. In another family with autosomal recessive hypoparathyroidism, a donor splice site mutation at the exon 2–intron 2 junction of the *PTH* gene was identified (13). The mutation leads to exon skipping and loss of exon 2 containing the initiation codon and signal sequence of preproPTH mRNA. In a few instances of autosomal dominant disease, a mutation in the *PTH* gene has been found. In one family, a missense mutation (C18R) in the signal sequence was identified (14), and the mutant was shown to be defective *in vitro* in

Table 1. Biochemical and Genetic Features of Patients With *PTH* Mutations

Index Case	Serum Calcium[a]	Serum Phosphate[a]	Serum PTH[a]	*PTH* Mutation	Heterozygous, Homozygous, Other	Familial	Reference
Infant male	1.8 mmol/L (2.1–2.6)[b]	1.5 mmol/L (0.8–1.5)	0.46 ng/mL (0.5–1.6)	c.52T>C p.C18R	Heterozygous	Yes	Arnold *et al.* (14), 1990
Female	NA	NA	NA	c.86+1G>Cexon 2 skipped	Homozygous	Yes	Parkinson *et al.* (13), 1992
Female, 7 days old	1.5 mmol/L (2.0–2.5)	3.6 mmol/L (0.9–1.5)	NA	c.67T>C p.S23P	Homozygous	Yes	Sunthornthepvarakul *et al.* (10), 1999
Female, 59 years old	11.8 mg/dL (8.8–10.2)	2.8 mg/dL (2.4–4.4)	Undetectable	c.247C>T p.R83X	Somatic[b]; hemizygous	No	Au *et al.* (16), 2008
Female, 4 months old	1.5 mmol/L (2.3–3.3)	3.7 mmol/L (1.6–2.6)	2.1 pg/mL (15–65)	c.68C>A p.S23X	Homozygous	Yes	Ertl *et al.* (11), 2012
Female, 18 years old	7.3 mg/dL (8.1–10.4)	6.9 mg/dL (2.5–4.5)	5.3 pg/mL (15–65)	c.2T>C p.M1_D6del	Heterozygous	No	Tomar *et al.* (15), 2013
Male, early adolescence	4.8 mg/dL (8.2–10-8)	8.1 mg/dL (2.5–4.7)	<5 pg/mL (10–65)	c.166C>T p.R56C	Homozygous	Yes	Lee *et al.* (12), 2015
Male, 2 years old	6.7 mg/dL (8.5–10.7)	10.3 mg/dL (4–7)	4.6 pg/mL (10–65)	c.41T>A p.M14K	Heterozygous	Yes	Present study

Abbreviation: NA, not available.

[a]Normal range in parentheses.

[b]Parathyroid tissue.

the processing of preproPTH to proPTH (17). Because the patients had one normal gene copy, the autosomal dominant mode of inheritance remained unclear until further studies in transfected cells proposed that the mutant was trapped in the ER, promoting ER stress and apoptosis (18). In another hypoparathyroid patient, a heterozygous M1T mutation was found, predicting for loss of Met1_Asp6 and abnormal translation initiation of the mutant preproPTH mRNA at the +7 Met codon (15).

In the present study, we identified a heterozygous M14K mutation in the signal peptide encoded by the *PTH* gene in the affected members of a three-generation family with FIH.

Patients and Methods

Case report

The proband, individual III-2 [Fig. 1(A)], was a male child born at term by spontaneous vaginal delivery, with a birth weight of 3380 g. His Apgar score was 10 at 1 minute and at 5 minutes. The infant's initial examination was unremarkable, his perinatal course was uneventful with no feeding problems and stable, and he was discharged at 3 days of life. The parents were nonconsanguineous. The personal and family histories of the father, individual II-3 [Fig. 1(A)] were unremarkable. However, hypoparathyroidism had been diagnosed in the mother, individual II-2 [Fig. 1(A)], the maternal grandmother, individual I-2 [Fig. 1(A)], and a maternal aunt, individual II-1 [Fig. 1(A)]. The grandmother, during childhood, had experienced convulsive episodes associated with low serum calcium and high phosphate levels, although she had not been treated for the underlying disease at that time, because hypoparathyroidism had been diagnosed only later. At 22 years of age, during her first pregnancy, she presented with status epilepticus and coma. Her female newborn, individual II-1 [Fig. 1(A)], died on the fifth day of life of severe hypocalcemic seizures. From that time onward, the grandmother took oral calcium carbonate (1 g/d) and calcitriol (0.5 μg/d) and has not experienced any further crises. Her serum PTH levels have been at the limit of detection (0.1 pg/mL; Access® Intact PTH; Beckman Coulter, Fullerton, CA), and her serum calcium and phosphate levels were 9.0 to 9.2 mg/dL and 4.0 to 4.1 mg/dL, respectively. During her second pregnancy, the doses of oral calcium and calcitriol were tripled, and she delivered, without complications, a female child (the mother of the proband). The newborn presented with neonatal hypocalcemic, normocalciuric, seizures, was diagnosed with hypoparathyroidism, and oral calcium carbonate and active vitamin D were started. At the time of the study, she was 31 years old and took 2 g/d of calcium carbonate and 1 μg/d of calcitriol. Her serum PTH values were undetectable (<0.1 pg/mL), and her serum calcium and phosphate levels were 8.2 to 8.5 mg/dL and 3.9 to 4.5 mg/dL, respectively. Her urinary calcium levels had been in the normal range (NR) for years (240 mg/24 hours). However, at the last evaluation, a higher value of 384 mg/24 hours was noted, which could indicate impaired renal calcium reabsorption becoming more apparent over time.

The proband, individual III-2 [Fig. 1(A)], presented on the sixth day of life for blood biochemical analysis because of the family history and flexor hypertonia. The infant's serum total

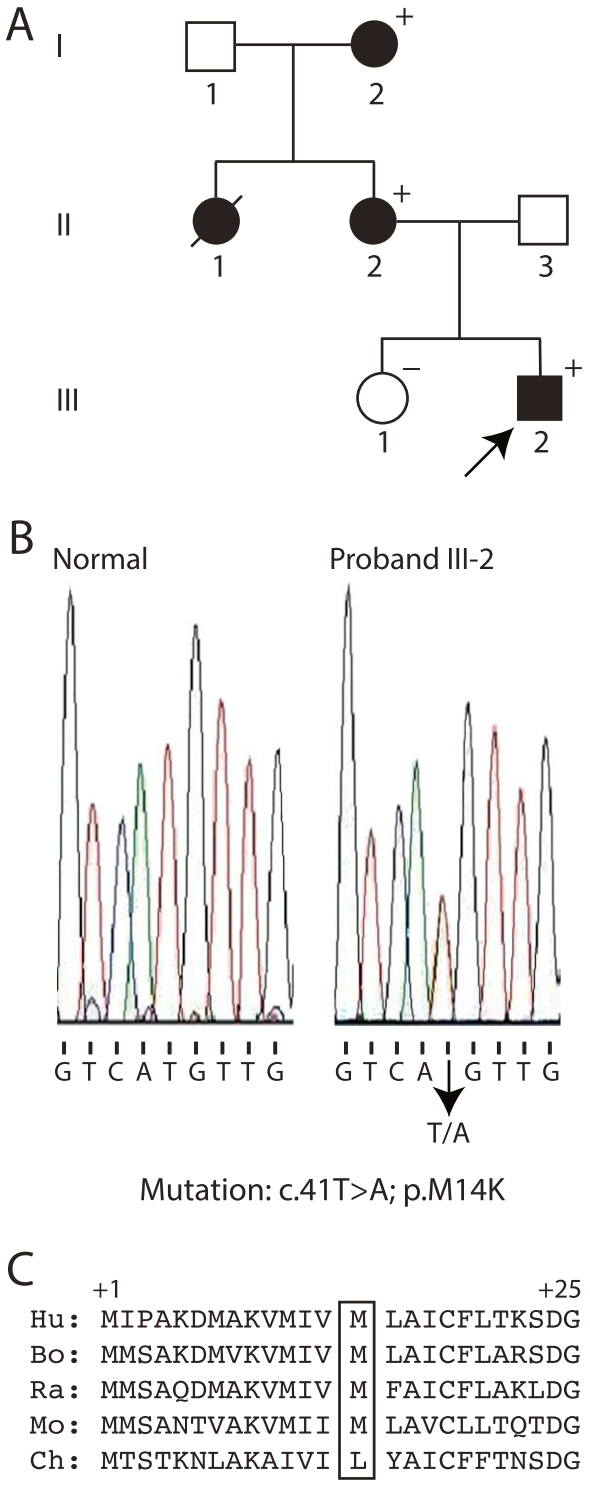

Figure 1. Detection of a mutation in the *PTH* gene. (A) Pedigree of family with FIH and *PTH* gene mutation: white symbol, unaffected or unknown; black symbol, affected. Proband is indicated by the arrow. The presence (+) or absence (−) of the mutation in family members is shown. (B) Direct sequence analysis of the PTH gene exon 2 amplicon showing a heterozygous T to A change encoding the missense M14K mutant in (Right) the proband (individual III-2) compared with (Left) an unrelated normal individual. (C) The PTH signal peptide sequences from diverse species were aligned as described in the Patients and Methods section. The residue corresponding to the M14K mutant is boxed. Abbreviations: Bo, bovine; Ch, chicken; Hu, human; Mo, mouse; Ra, rabbit.

calcium level was low, 6.7 mg/dL (NR, 8.5 to 10.7), serum phosphate level high, 10.3 mg/dL (NR, 4 to 7) and serum PTH level low, 4.8 pg/mL (NR, 10 to 65). Oral elemental calcium and calcifediol was started to restore the infant's blood concentrations of calcium and phosphate, and the family was referred to the pediatric division of the hospital. His thyroid function, blood count, immunoglobulins, and echocardiography findings were normal. Low serum PTH was confirmed (excluding transient neonatal hypoparathyroidism) and, at 8 months of age, was still 4.8 pg/mL. At the proband's last follow-up visit, the therapy was daily oral calcium and calcitriol. His growth has been normal (25th percentile using the World Health Organization height and weight chart), consistent with mid-parental height. Also, the infant was normal neurodevelopmentally. The proband's healthy 3-year-old sister, individual III-1 [Fig. 1(A)], has had normal serum calcium, phosphate, and PTH levels.

DNA sequence analysis

The subjects or their guardians provided written informed consent in accordance with the protocols approved by the local institutional ethics committee. DNA was extracted from blood leukocytes, and molecular screening of the *CASR*, *GNA11*, and *GCM2* gene protein-coding exons was performed, as described previously (19–21). For screening of the *PTH* gene, polymerase chain reaction (PCR) amplification of coding exons 2 and 3 and flanking sequence (22), using primer sequences in intron 1 (forward: 5′-GAGGTTGATTCCAAAAGC-3′) and in the gene 3′ flanking sequence (reverse: 5′-GCGTCCAGATTAGAACTATG-3′), was performed with the Expand Long Template PCR System (Roche, Mannheim, Germany), following the manufacturer's instructions. The amplicon was purified (ExoSAP-IT; Affymetrix, Santa Clara, CA) and directly sequenced with forward and reverse primers (Big Dye Terminator Sequencing Kit; Thermo Fisher, Waltham, MA). The mutation found in the *PTH* gene was confirmed by sequencing in both directions using different PCR products.

Public databases, the Single Nucleotide Polymorphism Database (available at: https://www.ncbi.nlm.nih.gov/projects/SNP/) and the Exome Aggregation Consortium (Cambridge, MA; available at: http://exac.broadinstitute.org/), were examined for the presence of the identified sequence variant. Phylogenetic conservation was evaluated using the MUSCLE (multiple sequence comparison by log-expectation) online tool (available at: http://www.ebi.ac.uk/Tools/msa/muscle/). The likelihood of a particular sequence functioning properly as a signal peptide and being cleaved appropriately was evaluated using the SignalP, version 4.1, server (available at: http://www.cbs.dtu.dk/services/SignalP/) (23, 24).

Site-directed mutagenesis

A Myc–FLAG-tagged human wild-type (WT) PTH complementary DNA (cDNA) expressing pCMV6 vector (catalog no. RC219848; Origene, Rockville, MD) was used as a template to generate mutants using our previously described methods (19). Sequences of the mutagenesis primers are available on request.

Transient transfection and western blot

Human embryonic kidney (HEK293) cells from the European Collection of Authenticated Cell Cultures (ECACC, Salisbury, UK) were seeded in six-well plates (19) and transfected with vectors using Fugene Transfection Reagent (Promega, Madison, WI), following the manufacturer's instructions. Total cell proteins were extracted in radioimmunoprecipitation assay buffer (150 mM NaCl, 50 mM Tris-HCl, 1% Nonidet P-40, 0.1% sodium dodecyl sulfate, 0.5% sodium deoxycholate, pH 8.0) supplemented with PhosStop and Complete EDTA, phosphatase and protease inhibitors (1 tablet/10 mL; both from Roche). Next, 80 μg of protein was separated by 8% sodium dodecyl sulfate-polyacrylamide gel electrophoresis, electrotransferred to polyvinylidene difluoride membrane (Millipore, Billerica, MA), incubated overnight at 4°C with primary monoclonal antibody and for 1 hour at room temperature with secondary antibody. The membranes were stripped and reprobed for the loading control. The primary antibodies were mouse anti-Myc (catalog no. 05-419; 1:1000 in blocking solution; Millipore) and rabbit anti–β-actin monoclonal antibody (catalog no. MAB12828; 1:1000 in blocking solution; Abnova, Taiwan). The secondary antibodies were horseradish peroxidase–conjugated goat anti-rabbit or anti-mouse IgG antibodies (1:5000 in blocking solution; Santa Cruz Biotechnology, Dallas, TX).

Culture media PTH levels

Cell culture media PTH levels were measured by the EIA Kit (catalog no. RAB0412; Sigma-Aldrich, Saint Louis, MO), following the manufacturer's instructions.

4-Phenylbutyric acid

Twenty-four hours after transfection of cells, 4-phenylbutyric acid (PBA; code 8209860025; Merck-Millipore, Billerica, MA) in water (or water alone) was added to a final concentration of 4 mM and culture of the cells was continued for another 48 or 72 hours.

Reverse transcription quantitative PCR

The *PTH* to *GAPDH* mRNA ratio was determined using our previously described methods (25). In brief, HEK293 cells were seeded in six-well plates and transfected with the WT, M14K, or C18R vectors. Forty-eight hours after 4-PBA stimulation (see previous section), the cells were detached, and RNA was extracted with Trizol (Qiagen, Hilden, Germany). First-strand cDNA synthesis from 1 μg of total RNA was performed with SuperScript III First-Strand Synthesis (Thermo Fisher). SYBR Green-based reverse transcription PCR was performed in a 10-μL reaction with iTaq Universal SYBR Green Supermix 2× (BioRad, Hercules, CA) using 1 μL of template cDNA and 1.2 mM and forward gene-specific primers. The range from 1×10^6 to 1×10^2 copies was used to build a standard curve of five serial plasmid dilutions. PTH construct mRNA levels were normalized to those of the endogenous *GAPDH* gene. The primers for *GAPDH* were as follows: 5′-GAAGGTGAAGGTCGGAGTC-3′ (forward) and 5′-GAAGATGGTGATGGGATTTC-3′ (reverse) and primers for the PTH cDNA were as follows: 5′-AAAAGTCTTGGAGAGGCAGACAAA-3′ (forward) (PTH sequence) and 5′-GAGATGAGTTTCTGCTCGAGCGGC-3′ (reverse) (Myc–FLAG-tag sequence). The cycling conditions were 10 minutes at 95°C, 50 cycles at 95°C for 15 seconds, and 60°C for 60 seconds. Reactions were run in triplicate on an ABIPRISM 7900HT (Applied Biosystems, Foster City, CA).

Statistical analysis

Data are expressed as the mean ± standard deviation. Statistical analyses were performed using the unpaired Student

t test with SAS, release 9.1 (SAS Institute, Cary, NC). A P value < 0.05 was considered statistically significant. The National Institutes of Health image processing program ImageJ (available at: http://rsb.info.nih.gov/ij/) was used for signal densitometry.

Results

Identification of PTH mutation

No mutations were detected in the *CASR*, *GCM2*, and *GNA11* genes of PCR-amplified genomic DNA from proband III-2 [Fig. 1(A)]. However, a heterozygous variant (c.41T>A; pM14K) in the signal peptide encoded by exon 2 of the *PTH* gene was identified [Fig. 1(B)]. A familial genetic analysis confirmed the segregation of the variant with the phenotype [Fig. 1(A)]. The variant is not present in either the Single Nucleotide Polymorphism Database or Exome Aggregation Consortium database, making the possibility that the variant is a rare polymorphism very unlikely. A phylogenetic analysis showed that methionine at residue 14 is highly conserved among orthologs and therefore likely to be of functional significance [Fig. 1(C)].

Mutant M14K lies within the hydrophobic core of the PTH signal peptide

Signal peptides have three essential conserved regions, the N-terminal, the n-region; the hydrophobic core, the h-region, critical for cotranslational processing; and the C-terminal, c-region, which ends at the signal peptide cleavage site. The sequence of the N-terminal 31 amino acids of preproPTH was examined using the SignalP hidden Markov model program. The program predicted a signal peptide (probability, 0.926) and not a signal anchor (probability, 0.036) with a cleavage site probability of 0.894 between positions +25 and +26 [Fig. 2(A) and 2(B)]. The PTH signal peptide is predicted to have an n-region from amino acid 1 to 9, an h-region from amino acid 10 to 20, and a c-region from amino acid 21 to 25 [Fig. 2(A) and 2(B)].

M14K substitution is inconsistent with signal peptide function and cleavage

The SignalP neural network program is a useful tool to evaluate *in silico* whether particular variant amino acids in a signal sequence are consistent with function. The analysis yields the s-score, which reports the signal peptide prediction for every single amino acid position, with high scores indicating that the particular amino acid is part of a functioning signal peptide. The c-score is the cleavage site score, with the cleavage site position identified. The y-score is a derivative of the c-score combined with the s-score, resulting in more accurate cleavage site prediction. For the PTH WT presequence (+1 to +25), the mean s-score was 0.623, with no amino acid less than the 50% cutoff [Fig. 3(A)]. However, the mean s-score for the M14K mutant was 0.373 [Fig. 3(B)] and for the previously described C18R mutant was 0.437 [Fig. 3(C)], well below the 50% cutoff. For WT, M14K, and C18R, the maximum y-scores were 0.591, 0.391, and 0.376, respectively. Thus, although the scores for the WT sequence were fully consistent with function as a signal peptide (and cleavage between amino acids +25 and +26), those of M14K and C18R were not consistent with signal peptide function and cleavage.

Transfected M14K mutant is retained intracellularly in HEK293 cells

By site-directed mutagenesis, c-Myc–tagged M14K and C18R mutant expression constructs were created and transiently transfected into HEK293 cells, as was the c-Myc–tagged WT vector. Western blot analysis was conducted with an antibody against the c-Myc epitope tag. This showed that much higher levels of the M14K and C18R mutants were present intracellularly relative to that of WT after 48 and 72 hours of culture [Fig. 4(A–D), Left]. In contrast, although high levels of WT PTH were released into the cell media after 48 hours, very little PTH was present in the media of cells transfected with the M14K and C18R mutants [Fig. 5].

4-PBA reduces the intracellular accumulation of the M14K mutant

Culture of HEK293 cells, transiently transfected with the PTH constructs, with the chemical chaperone, 4-PBA, led to a marked reduction in intracellular expression of immunoreactive PTH for the mutants; 9-fold in the case of M14K and 16-fold in the case of C18R at 48 hours [Fig. 4(A) and 4(B); Right] relative to culture without 4-PBA [Fig. 4(A) and 4(B); Left). This effect was still evident, although to a lesser extent after 72 hours of culture [Fig. 4(C) and 4(D)]. Although the culture of cells transfected with the WT construct with 4-PBA increased the already high levels of PTH in the media only modestly, the levels in the media of cells transfected with the mutants were markedly increased; 15-fold in the case of M14K and 21-fold in the case of C18R, relative to cells not treated with 4-PBA.

4-PBA has no or modest effect on PTH construct transcript levels

One of the proposed actions of 4-PBA is as a histone deacetylase inhibitor, and this action might alter expression of the PTH constructs in an indirect way. The effect of 4-PBA on the PTH transcript levels in the HEK293 cells transfected with the various constructs was evaluated by reverse transcription quantitative PCR analysis of RNA isolated from cells cultured for 48 hours. The *PTH/GAPDH* mRNA levels under 4-PBA nontreated

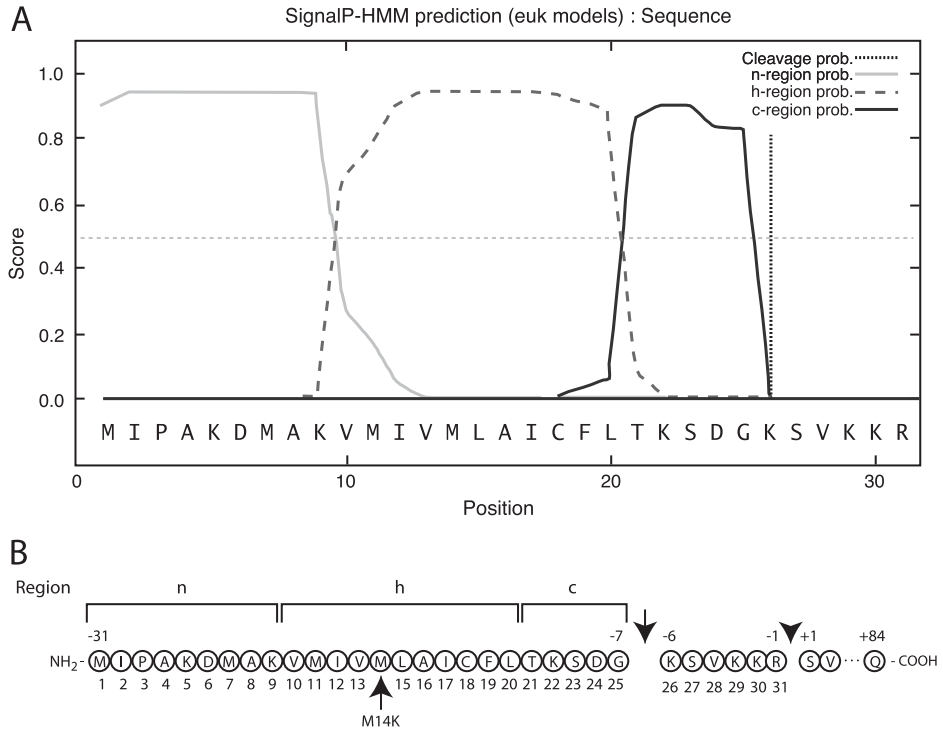

Figure 2. (A) An evaluation of the N-terminal region of preproPTH as a signal peptide was made using the SignalP hidden Markov model program (version 3.0). A highly relevant probability (prob.) score was obtained, and the positions of the n-, h-, and c-regions were predicted, in addition to a signal peptide cleavage site between amino acids 25 and 26. (B) A summary of the SignalP predictions. Bracketed sequences indicate the predicted n-, h-, and c-regions. Residues are numbered conventionally, with the first residue (S) of the mature PTH polypeptide designated as +1 and the last residue (Q) as +84, and the pre (signal)-peptide as −31 to −7 and the propeptide as −6 to −1. The signalase cleavage site is indicated by the arrow, and the proprotein convertase cleavage site is indicated by the arrowhead. In addition, the initiation codon methionine residue is alternatively designated as +1, and the M14K mutation is indicated by the arrow.

vs treated conditions were as follows: WT, 100 ± 4 vs 108 ± 12 (mean ± standard deviation; P = NS); M14K, 106 ± 12 vs 146 ± 8 ($P < 0.05$); and C18R, 93 ± 8 vs 137 ± 4 ($P < 0.05$). Thus, 4-PBA had only a modest effect on the exogenous expression of PTH driven by the transfected mutant constructs, and this did not account for the relatively large increase in secretion of PTH into cell media stimulated by 4-PBA treatment.

Discussion

To date, a few *PTH* mutations have been identified as the genetic cause of hypoparathyroidism inherited in either an autosomal dominant or a recessive fashion (Table 1). For the recessive forms, nearly complete hormone insufficiency explains the disease. In the case of the first heterozygous *PTH* mutation (C18R) identified (14), the clinical expression of hypoparathyroidism in the presence of one WT *PTH* allele was not immediately obvious. Extensive *in vitro* analyses confirmed that the mutation induced impairment at multiple stages of PTH processing and maturation but were unable to document a dominant negative effect of the mutant on WT (15). A further *in vitro* study showed that the mutation caused accumulation of immunoreactive PTH within the cell promoting ER stress, leading to apoptosis and, thus, providing an explanation for the hypoparathyroidism (18).

We report on a three-generation FIH family with low to undetectable circulating PTH levels. No mutations were detected in the *CASR*, *GCM2*, and *GNA11* genes of the patients. However, a heterozygous variant (c.41T>A; pM14K) in the signal peptide encoded by exon 2 of the *PTH* gene was identified that segregated with affected status in the family. Query of publicly accessible single nucleotide polymorphism databases suggested that the variant is not a rare polymorphism. A phylogenetic analysis showed that methionine +14 is highly conserved and likely to be of functional significance.

The SignalP bioinformatics tool proved helpful in evaluating potential functional effects of natural mutations in signal sequences [*e.g.*, Pidasheva *et al.* (26)]. In the present study, we used the most recent SignalP version (version 4.1) to evaluate the WT and M14K and C18R mutant presequences. Thus, although the scores for the WT sequence were fully consistent with function as a signal peptide, interaction with the signal recognition particle, translocation into the lumen of the ER, and cleavage by the signalase enzyme between amino acids +25 and +26, those of M14K and C18R were not consistent with proper signal peptide function and cleavage.

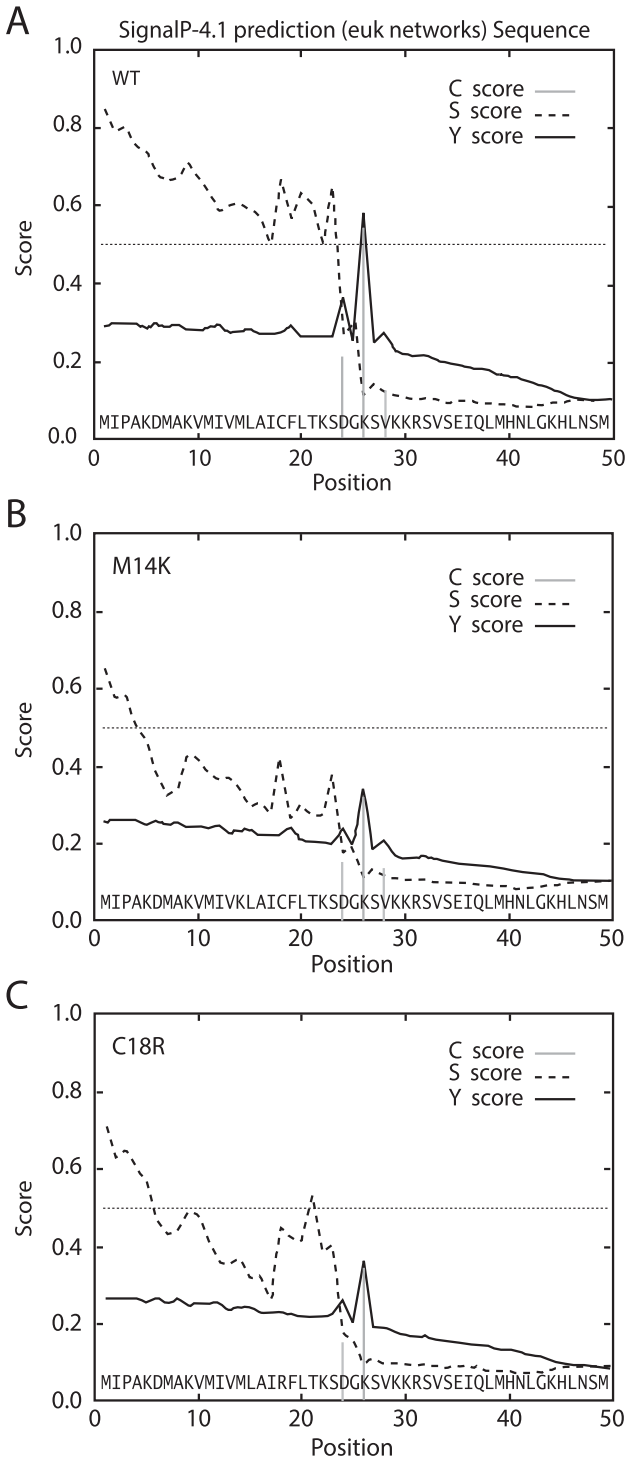

Figure 3. Comparison of the signal peptides of preproPTH WT and mutants. The NH_2-terminal regions of (A) preproPTH WT and mutants (B) M14K and (C) C18R were analyzed with the SignalP-neural network program (version 4.1). Attainment of signal peptide prediction (s−), cleavage site prediction (c−), and derived cleavage site prediction (y−) scores more than the 50% cutoff indicate proper signal peptide function and cleavage, and values less than the cutoff indicate compromised function.

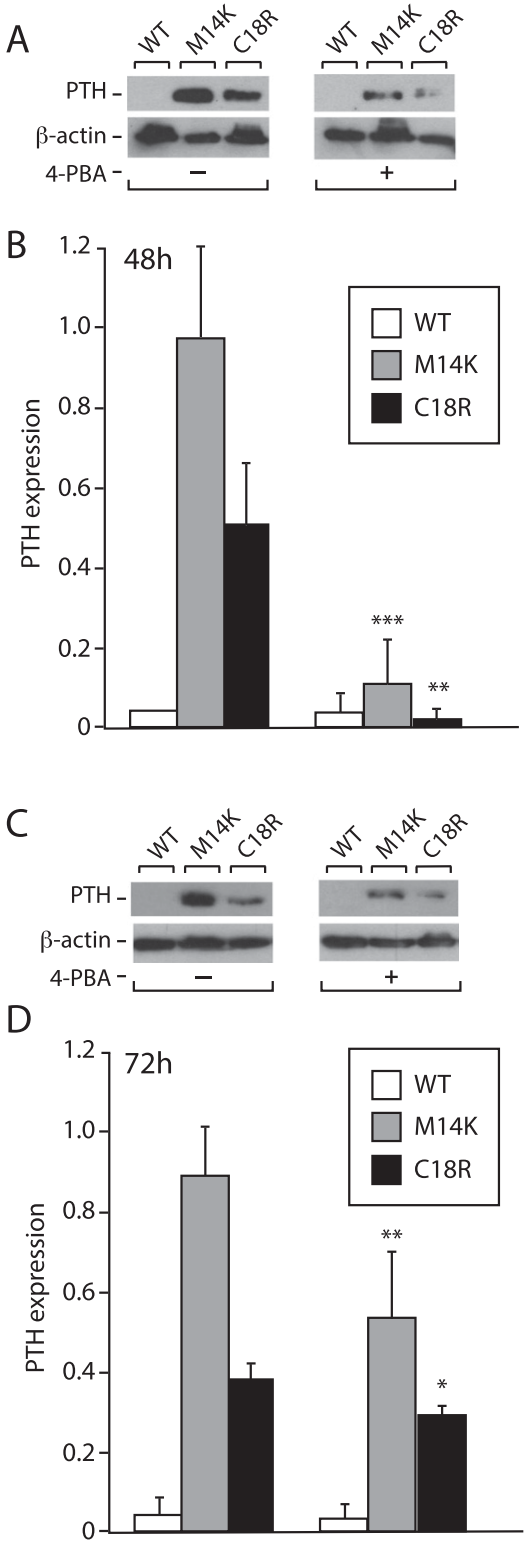

Figure 4. Western blot analysis of cell extracts of HEK293 cells transiently transfected with WT or mutant (M14K or C18R) c-myc–tagged PTH constructs and treated (+) or not (−) with 4 mM 4-PBA for (A and B) 48 hours or (C and D) 72 hours. (A and C) Recombinant proteins were stained with c-Myc monoclonal antibody, and endogenous proteins were stained with a β-actin antibody. (B and D) Levels of the tagged PTH species (WT, M14K, and C18R) relative to β-actin were determined by densitometry. Data are presented as the mean ± standard deviation of triplicate experiments. $*P < 0.05$, $**P < 0.01$, and $***P < 0.001$ compared with the corresponding condition not treated with 4-PBA.

The results of our *in vitro* functional assays indicated that in HEK293 cells transfected with the WT construct, proper secretion of PTH into the medium occurred and

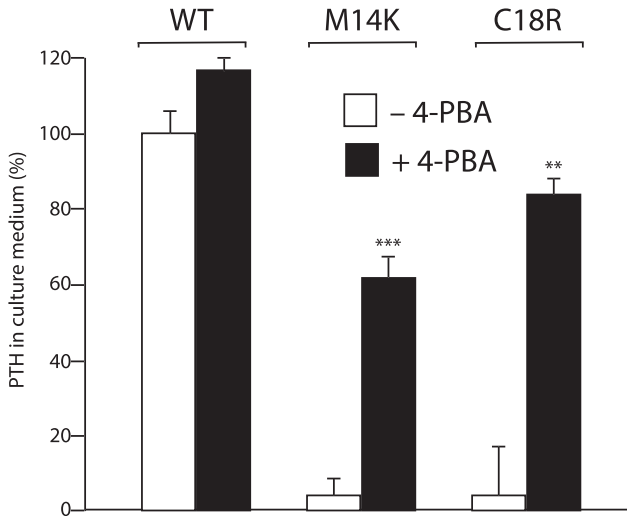

Figure 5. PTH enzyme-linked immunosorbent assay of media of HEK293 cells transiently transfected with WT or mutant (M14K or C18R) c-myc–tagged PTH constructs and treated (+) or not (−) with 4 mM 4-PBA for 48 hours. Data are presented as the mean ± standard deviation of triplicate experiments. $^{**}P < 0.01$ and $^{***}P < 0.001$ compared with corresponding condition not treated with 4-PBA.

rather little immunoreactive-tagged PTH was present intracellularly, indicating appropriate processing. In contrast, in the cells transfected with either the M14K or C18R constructs, marked accumulation of an immunoreactive 14-kDa form of tagged PTH was found by western blot intracellularly and very little immunoreactive PTH was present in the cell media. Using confocal fluorescence microscopy (data not shown), marked accumulation of immunoreactive-tagged PTH occurred in the cells transfected with the mutant M14K construct.

4-PBA is a short-chain fatty acid that functions as a pharmacological chaperone and histone deacetylase inhibitor (27). It can exert a direct action on misfolded proteins within the ER, thus reducing ER stress and cell apoptosis. In addition, its ability to relax chromatin structure enhances the transcription of genes for endogenous chaperones such as heat shock proteins (27). 4-PBA has been approved by the Food and Drug Administration for treatment of an unrelated metabolic urea cycle disorder, and clinical trials for its use in cancer, blood, and neurodegenerative disease are ongoing (27). We explored whether 4-PBA, already reported to be able to correct the trafficking of the C18R mutant (18), was likewise effective with our M14K mutant. In the present study, we confirm the efficacy of 4-PBA in ameliorating the intracellular accumulation of the C18R mutant and restoring the secretion of PTH. We also found the same effect for the M14K mutant of the present study. Thus, although not directly addressed in our study, the M14K mutant might well exert similar effects as the C18R mutant by stimulating cellular stress and apoptosis. The ability of the chemical chaperone 4-PBA to restore secretion of PTH toward normal suggests its possible clinical use for protein trafficking disorders such as the one under discussion.

Finally, although supplementation with calcium and active vitamin D, such as for the patients of our family with a *PTH* mutation is appropriate, the urinary calcium excretion became high for the proband's mother. This deserves clinical monitoring for the possible risks of nephrocalcinosis, nephrolithiasis, and renal damage, complications that are instead very common in cases with an activating *CASR* mutation. Thus, the differential molecular diagnosis in patients with FIH is important for clinical management and genetic counseling.

Acknowledgments

We thank the family participating in the present study.

Financial Support: This research was supported by Ricerca Corrente funding granted by the Italian Ministry of Health (to V.G.), the "5x1000" voluntary contributions, and the Mauro Baschirotto Institute for Rare Diseases Foundation. The funders had no role in the study design or collection, analysis, and interpretation of the data or writing the manuscript.

Correspondence and Reprint Requests: Paolo Prontera MD, PhD, Servizio di Genetica Medica, "Santa Maria della Misericordia" Hospital, Piazzale Menghini, 8/9, Edificio CREO, Perugia, Italy. E-mail: paolo.prontera@ospedale.perugia.it.

Disclosure Summary: The authors have nothing to disclose

References

1. Shoback DM, Bilezikian JP, Costa AG, Dempster D, Dralle H, Khan AA, Peacock M, Raffaelli M, Silva BC, Thakker RV, Vokes T, Bouillon R. Presentation of hypoparathyroidism: etiologies and clinical features. *J Clin Endocrinol Metab*. 2016;**101**(6):2300–2312.
2. Hendy GN, Cole DEC, Bastepe M. Hypoparathyroidism and pseudohypoparathyroidism. In De Groot LJ, Chrousos G, Dungan K, Feingold KR, Grossman A, Hershman JM, Koch C, Korbonits M, McLachlan R, New M, Purnell J, Rebar R, Singer F, Vinik A, eds. *Endotext [Internet]*. South Dartmouth, MA: MDText.com, Inc.; 2000-2017 Feb 19.
3. Hendy GN, Cole DEC. Familial isolated hypoparathyroidism. In: Brandi ML, Brown EM, eds. *Hypoparathyroidism*. Milan, Italy: Springer-Verlag Italia; 2015:167–175.
4. Hannan FM, Babinsky VN, Thakker RV. Disorders of the calcium-sensing receptor and partner proteins: insights into the molecular basis of calcium homeostasis. *J Mol Endocrinol*. 2016;**57**(3): R127–R142.
5. Roszko KL, Bi RD, Mannstadt M. Autosomal dominant hypocalcemia (hypoparathyroidism) types 1 and 2. *Front Physiol*. 2016; 7:458.
6. Günther T, Chen Z-F, Kim J, Priemel M, Rueger JM, Amling M, Moseley JM, Martin TJ, Anderson DJ, Karsenty G. Genetic ablation of parathyroid glands reveals another source of parathyroid hormone. *Nature*. 2000;**406**(6792):199–203.
7. Ding C, Buckingham B, Levine MA. Familial isolated hypoparathyroidism caused by a mutation in the gene for the transcription factor GCMB. *J Clin Invest*. 2001;**108**(8):1215–1220.
8. Mannstadt M, Bertrand G, Muresan M, Weryha G, Leheup B, Pulusani SR, Grandchamp B, Jüppner H, Silve C. Dominant-negative

GCMB mutations cause an autosomal dominant form of hypoparathyroidism. *J Clin Endocrinol Metab*. 2008;**93**(9):3568–3576.
9. Canaff L, Zhou X, Mosesova I, Cole DE, Hendy GN. Glial cells missing-2 (GCM2) transactivates the calcium-sensing receptor gene: effect of a dominant-negative GCM2 mutant associated with autosomal dominant hypoparathyroidism. *Hum Mutat*. 2009; **30**(1):85–92.
10. Sunthornthepvarakul T, Churesigaew S, Ngowngarmratana S. A novel mutation of the signal peptide of the preproparathyroid hormone gene associated with autosomal recessive familial isolated hypoparathyroidism. *J Clin Endocrinol Metab*. 1999;**84**(10): 3792–3796.
11. Ertl DA, Stary S, Streubel B, Raimann A, Haeusler G. A novel homozygous mutation in the parathyroid hormone gene (PTH) in a girl with isolated hypoparathyroidism. *Bone*. 2012;**51**(3):629–632.
12. Lee S, Mannstadt M, Guo J, Kim SM, Yi HS, Khatri A, Dean T, Okazaki M, Gardella TJ, Jüppner H. A homozygous [Cys25]PTH(1-84) mutation that impairs PTH/PTHrP receptor activation defines a novel form of hypoparathyroidism. *J Bone Miner Res*. 2015;**30**(10): 1803–1813.
13. Parkinson DB, Thakker RV. A donor splice site mutation in the parathyroid hormone gene is associated with autosomal recessive hypoparathyroidism. *Nat Genet*. 1992;**1**(2):149–152.
14. Arnold A, Horst SA, Gardella TJ, Baba H, Levine MA, Kronenberg HM. Mutation of the signal peptide-encoding region of the preproparathyroid hormone gene in familial isolated hypoparathyroidism. *J Clin Invest*. 1990;**86**(4):1084–1087.
15. Tomar N, Gupta N, Goswami R. Calcium-sensing receptor autoantibodies and idiopathic hypoparathyroidism. *J Clin Endocrinol Metab*. 2013;**98**(9):3884–3891.
16. Au AYM, McDonald K, Gill A, Sywak M, Diamond T, Conigrave AD, Clifton-Bligh RJ. PTH mutation with primary hyperparathyroidism and undetectable intact PTH. *N Engl J Med*. 2008; **359**(11):1184–1186.
17. Karaplis AC, Lim SK, Baba H, Arnold A, Kronenberg HM. Inefficient membrane targeting, translocation, and proteolytic processing by signal peptidase of a mutant preproparathyroid hormone protein. *J Biol Chem*. 1995;**270**(4):1629–1635.
18. Datta R, Waheed A, Shah GN, Sly WS. Signal sequence mutation in autosomal dominant form of hypoparathyroidism induces apoptosis that is corrected by a chemical chaperone. *Proc Natl Acad Sci USA*. 2007;**104**(50):19989–19994.
19. Guarnieri V, Valentina D'Elia A, Baorda F, Pazienza V, Benegiamo G, Stanziale P, Copetti M, Battista C, Grimaldi F, Damante G, Pellegrini F, D'Agruma L, Zelante L, Carella M, Scillitani A. CASR gene activating mutations in two families with autosomal dominant hypocalcemia. *Mol Genet Metab*. 2012;**107**(3):548–552.
20. D'Agruma L, Coco M, Guarnieri V, Battista C, Canaff L, Salcuni AS, Corbetta S, Cetani F, Minisola S, Chiodini I, Eller-Vainicher C, Spada A, Marcocci C, Guglielmi G, Zini M, Clemente R, Wong BY, de Martino D, Scillitani A, Hendy GN, Cole DE. Increased prevalence of the GCM2 polymorphism, Y282D, in primary hyperparathyroidism: analysis of three Italian cohorts. *J Clin Endocrinol Metab*. 2014;**99**(12):E2794–E2798.
21. Stratta P, Merlotti G, Musetti C, Quaglia M, Pagani A, Izzo C, Radin E, Airoldi A, Baorda F, Palladino T, Leone MP, Guarnieri V. Calcium-sensing-related gene mutations in hypercalcaemic hypocalciuric patients as differential diagnosis from primary hyperparathyroidism: detection of two novel inactivating mutations in an Italian population. *Nephrol Dial Transplant*. 2014;**29**(10): 1902–1909.
22. Vasicek TJ, McDevitt BE, Freeman MW, Fennick BJ, Hendy GN, Potts JT Jr, Rich A, Kronenberg HM. Nucleotide sequence of the human parathyroid hormone gene. *Proc Natl Acad Sci USA*. 1983; **80**(8):2127–2131.
23. Petersen TN, Brunak S, von Heijne G, Nielsen H. SignalP 4.0: discriminating signal peptides from transmembrane regions. *Nat Methods*. 2011;**8**(10):785–786.
24. Bendtsen JD, Nielsen H, von Heijne G, Brunak S. Improved prediction of signal peptides: SignalP 3.0. *J Mol Biol*. 2004;**340**(4): 783–795.
25. Pazienza V, la Torre A, Baorda F, Alfarano M, Chetta M, Muscarella LA, Battista C, Copetti M, Kotzot D, Kapelari K, Al-Abdulrazzaq D, Perlman K, Sochett E, Cole DE, Pellegrini F, Canaff L, Hendy GN, D'Agruma L, Zelante L, Carella M, Scillitani A, Guarnieri V. Identification and functional characterization of three NoLS (nucleolar localisation signals) mutations of the CDC73 gene. *PLoS One*. 2013;**8**(12):e82292.
26. Pidasheva S, Canaff L, Simonds WF, Marx SJ, Hendy GN. Impaired cotranslational processing of the calcium-sensing receptor due to signal peptide missense mutations in familial hypocalciuric hypercalcemia. *Hum Mol Genet*. 2005;**14**(12):1679–1690.
27. Iannitti T, Palmieri B. Clinical and experimental applications of sodium phenylbutyrate. *Drugs R D*. 2011;**11**(3):227–249.